*International Journal of Remote Sensing*
Vol. 30, No. 11, 10 June 2009, 2859–2873

# Fusion of multi-spectral SPOT-5 images and very high resolution texture information extracted from digital orthophotos for automatic classification of complex Alpine areas

CLAUDIO MARIZ†‡, DAMIANO GIANELLE*†, LORENZO BRUZZONE‡ and LORIS VESCOVO†

†Centro di Ecologia Alpina, Fondazione E. Mach, Viote del Monte Bondone, I-38040, Trento, Italy

‡Department of Information Engineering and Computer Science, University of Trento, Via Sommarive, 14 I-38050, Povo, Trento, Italy



In areas with complex three-dimensional features, slope and aspect interact with light conditions and significantly affect the spatial structure of images acquired by remote sensing instruments (for example, by changing the distribution of shadows and affecting the texture of high resolution imagery). In this scenario, this paper analyses the potential and the effectiveness of an automatic classification system to identify three fundamental vegetation classes (forest, grassland and crops) in the complex topography of the Italian Alps (Autonomous Province of Trento, Italy). This classification system is based on the fusion of spectral information provided by the SPOT-5 multi-spectral channels (Ground Instantaneous Field of View, GIFOV, equal to 10 m) and textural information extracted from airborne digital orthophotos (GIFOV equal to 1 m) and is designed to be user-friendly. The texture of the digital orthophotos was modelled using defined bidirectional variograms, thereby extracting additional information unavailable in first-order texture analyses. Using SPOT-5 multi-spectral information alone, the classification accuracy in the investigated alpine area was equal to 87.5%, but increased to 92.1% when texture information was included. In particular, the texture information significantly increased the classification accuracy for crops (from 68.9% to 87.9%), especially orchards that tend to be classified as lowland deciduous forests, and herbaceous crops (such as maize) that are often misclassified as grasslands. A further simple majority analysis increased the ability of detecting grassland, crops and urban zones. The combination of the majority analysis and the proposed automatic classification system seems an effective approach to classifying vegetation types in highly fragmented and complex Alpine landscapes on a regional scale.

## 1. Introduction

Remote sensing is used widely for land-use classification and forest inventory maps, as it is a relatively rapid, accurate and cost-effective method when applied to large areas, especially if integrated with automatic processing techniques. Several previous studies have investigated the potential of different remote sensors for estimating land cover and classifying vegetation, including passive multi-spectral and hyperspectral sensors, as well as active Light Detection and Ranging (LIDAR) and Synthetic Aperture Radar (SAR) systems (Hyde *et al.* 2006).

*Corresponding author. Email: gianelle@cealp.it

*International Journal of Remote Sensing*
ISSN 0143-1161 print/ISSN 1366-5901 online © 2009 Taylor & Francis
http://www.tandf.co.uk/journals
DOI: 10.1080/01431160802558600

Depending on the spectral and geometrical characteristics of the available multi-spectral sensors, classification can be achieved at different levels of detail. If low resolution multi-spectral data are available, analysis generally is limited to discriminating between forested and non-forested areas (Sedano *et al.* 2005). Instead, medium resolution sensors can increase the level of detail significantly and analysis can be focused on more specific vegetation classes, as shown by Goodenough *et al.* (2003), who used Landsat Enhanced Thematic Mapper Plus (ETM+) images to analyse eight different classes. High resolution orbital sensors, such as Quickbird, Ikonos and SPOT-5, allow the generation of geometrically detailed land-cover maps. However, due to technological limitations, the high spatial resolution of the images results in a decreased spectral resolution, which affects the classification accuracy (Zhang 2001). Consequently, in order to obtain thematic maps characterized by high accuracy, the development of novel algorithms is essential for allowing the available texture information to be incorporated into the classification process. In addition, in order to exploit all the information contained in high resolution images, it is necessary to consider both spectral reflectance and the three-dimensional spatial organization of the image (St-Onge and Cavayas 1995). In particular, texture contains important structural information that should be used in the classification process, since its variations are related to changes in spatial distribution of the objects in the scene (Wulder *et al.* 1998, Atkinson and Lewis 2000).

In fact, many studies have pointed out the usefulness of adding textural information to the classification process (Nel *et al.* 1994, Coburn and Roberts 2004, Ruiz *et al.* 2004, Zhang *et al.* 2004), and for the estimation of a number of biophysical parameters, such as Leaf Area Index (LAI; Wulder *et al.* 1998), wood volume and forest structure (St-Onge and Cavayas 1995), crown size and cover stratification (Cohen *et al.* 1990), and stem density or mean tree height (St-Onge and Cavayas 1995, Bruniquel-Pinet and Gastellu-Etchegorry 1998). Other studies have evaluated the relationships between high-resolution image semivariance image texture, and tree health (Lévesque and King 1999).

Several methods exist for extracting textural information from images, such as simple local variance measurements (Hsu 1978), second-order spatial statistics (Cohen *et al.* 1990) and neural network approaches (Dreyer 1993). These methods can be divided into structural, model-based and frequency-based approaches (see also Coburn and Roberts (2004) for greater details). One of the more widely used is the extraction of second-order statistics using variograms (Cohen *et al.* 1990, St-Onge and Cavayas 1997, Bruniquel-Pinet and Gastellu-Etchegorry 1998, Curran 1998, Lévesque and King 1999). In general, variograms provide information unobtainable by first-order texture analysis (St-Onge and Cavayas 1995), although recently Coburn and Roberts (2004) demonstrated that variance measured over various window sizes can be considered to be equivalent to the semivariance measure.

Wulder *et al.* (1998) suggested that homogeneous stands could be modelled with first-order texture measures, while heterogeneous stands can be characterized according to second-order texture measures and a semivariogram approach. These geostatistical tools allow variation in spatial correlation of the reflectance to be quantified. In particular, the use of variogram model parameters (such as range and sill) permits the identification and the quantification of the spatial characteristics of land surfaces (Chen and Gong 2004), species and cover type (Wulder *et al.* 1998). Miranda and Fonseca (1998) used the variogram to define a semivariogram textural algorithm (STC) for classifying flooded areas in the Amazon rainforest by using SAR data.

Variograms have also been used to determine the appropriate spatial resolution for studying ecological problems, or to evaluate the optimal sample plot size (Butson and King 1999). Franklin *et al.* (1996) used semivariograms to generate windows, which are customized to the scale of observations, in order to demonstrate improvement in remote estimation of forest parameters and in land-cover classification. Hese (2001) analysed the potential of directional variogram parameters in stand forest structure differentiation. However, there is still some uncertainty in the determination of texture measures, window size and other related parameters, and more research is needed to develop new methods for selecting texture parameters suitable for different biophysical environments (Lu and Weng 2007).

The importance of textural information for vegetation classification is particularly evident in cases where the use of spectral analysis is limited. For example, accurate estimates of biophysical parameters at full canopy cover have still not been fully achieved from multi-spectral data, as broad-band spectral vegetation indices tend to saturate and canopy biophysical characteristics ( e.g. LAI, biomass) have nonlinear relationships with a number of vegetation indices (such as the Normalized Difference Vegetation Index, NDVI) under these conditions (Lévesque and King 2003). Moreover, when tree canopy cover is low, the understorey component influences the response measured by a spectral sensor introducing errors in the computation of the biophysical parameters (Colombo *et al.* 2003). When these spectral indices fail, the application of textural indices offers potential for measuring and monitoring canopy structures (Hudak and Wessman 1998, 2001). In fact, the combination of spatial and spectral analysis was used successfully to solve this problem by Wulder *et al.* (1996, 1998) and Bruniquel-Pinet and Gastellu-Etchegorry (1998), who showed that the introduction of semivariogram texture improved the regression relationship between LAI and NDVI, especially at full canopy cover, when LAI values are greater than three.

The aim of this study was to apply an approach that integrates textural analysis of digital orthophotos (Ground Instantaneous Field of View (GIFOV) equal to 1 m) with SPOT-5 multi-spectral imagery information (GIFOV equal to 10 m) to the classification of vegetation in Alpine areas with a complex topography. The ultimate goal was to define an automatic classification method that jointly exploits the non-uniform and non-random spatial distribution of natural vegetation (modelled at very high geometrical resolution in orthophotos) and spectral information (acquired from SPOT-5 sensor) for the recognition of four fundamental land cover classes in Alpine areas: forest, grassland, crops, and urban areas.

## 2. Materials and methods

### 2.1 *Study area*

The study site (ca 52 km$^2$) is located in northern Italy, approximately 10 km south-east of Trento, in a typical alpine area. The lowest altitudes (300 m above sea level (asl)) are occupied by crops of grapes, apples and maize and some deciduous forest. Also included in the site is part of the Piana delle Viote, a wide plateau at 1550 m asl, dominated by grasslands (meadows and pastures), while the rest of the site is covered by mixed forest of beech and spruce. This location was selected in order to analyse a range of vegetation types in a very complex topography. Slope and aspect and their interactions with viewing direction and light conditions significantly affect the appearance of spatial structures in the image. In fact, the solar zenith and azimuth angles, in combination with slope and aspect, change the amount of the shadow projected on the ground and thus the shape of the variogram (i.e. change the value of range and sill).

### 2.2 *Data sources*

Two different data sources were considered in our study: a SPOT-5 image and a digital orthophoto. The SPOT-5 image was acquired on 27 April 2004, with a clear sky apart from a few small isolated clouds. It has four spectral bands and a spatial resolution of 10 m. The geographical location of the scene was $46^\circ 05'$ N (centre latitude), $10^\circ 43'$ E (centre longitude). The image was geometrically corrected, and georeferenced in a Universal Transverse Mercator (UTM) grid.

The digital orthophoto, a very high resolution image (GIFOV equal to 1 m) was acquired in the red, green and blue bands of the electromagnetic spectrum by a sensor mounted on an aerial platform in the summer of 2003 and was georeferenced, orthorectified and geometrically corrected.

One potential problem in integrating information from the two images used here is that some small areas of the SPOT-5 and the orthophoto images were incongruous, due to land-use changes that occurred on the ground between the two acquisition dates. In order to avoid these spurious effects in our analysis, before running the classification, multi-temporal images were compared and land-use change areas were excluded from the analysis.

An image with a resolution of 10 m was extracted from the orthophoto to match that of the SPOT-5 image using a nearest-neighbour resampling algorithm with a 0.1 factor band. The three spectral bands of the resulting orthophoto image, the textural features (range–sill), and the four SPOT-5 satellite channels were co-registered and a maximum root square registration error of 10 m was obtained. Figure 1 summarizes the information sources considered in the classification process.

### 2.3 *Texture analysis*

A spatial statistical approach based on the variogram was used to extract the structural information of the vegetation cover. This tool permits the characterization of the spatial structure of the scene, while being easy to implement and interpret.

The semivariance $\gamma$ can be defined as half the squared difference between the variable $Z$ (the variance, or in this case, the reflectance) calculated at two precise locations, $x$ and $x+h$.

$$\gamma^2 = \frac{1}{2}[Z(x) - Z(x+h)]^2 \tag{1}$$

The variogram $\gamma(h)$ is calculated with the following equation:

$$\gamma(h) = \frac{1}{2m} \cdot \sum_{i=1}^{m} [Z(x_i) - Z(x_i+h)]^2 \tag{2}$$

where $m$ is the number of pairs of pixels separated by the same lag($h$), and $Z(x_i)$ is the digital value at the $x_i$ position. This variable represents a measure of the degree

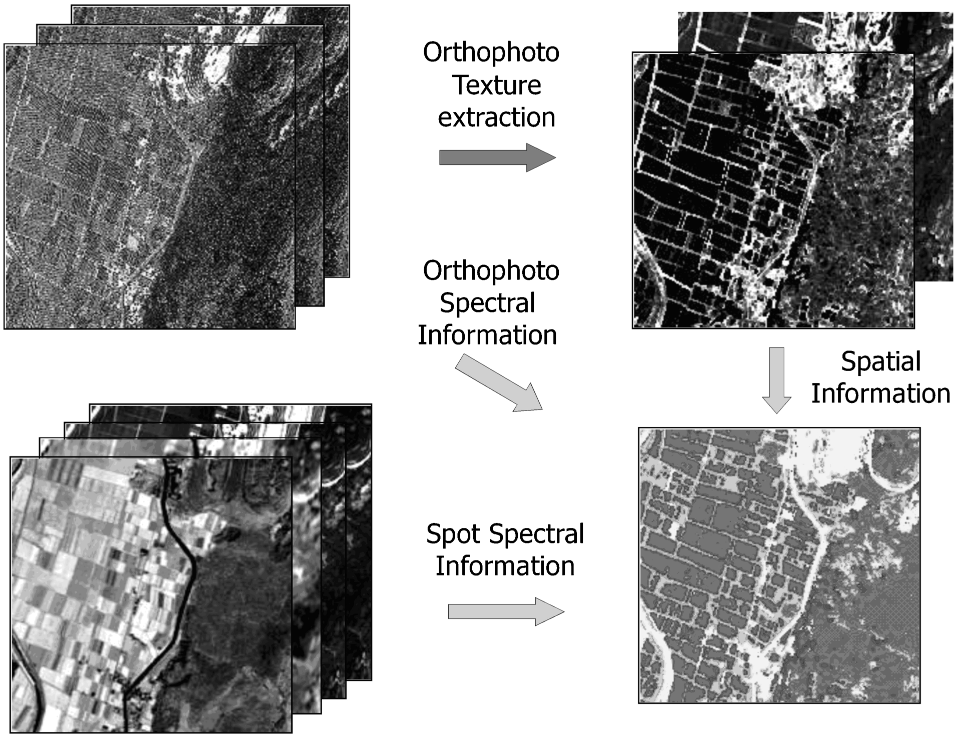


Figure 1. Information sources considered in the classification process: spectral information (SPOT-5 and orthophoto images) and texture information (extracted from the orthophoto). The image size is $1 \times 1$ km.



of spatial dependence between samples and can be defined as the plot of semivariance at different distances (Colombo *et al.* 2003).

The sill, nugget and range are the most important parameters that can be extracted from a variogram. The sill represents the height of the variogram (or the point at which the variogram tends to be horizontal), while the nugget is the interception with the coordinate axis. The range can be defined as the distance value at which the variogram reaches the sill and can be considered as the distance at which the observation becomes independent from the distance between samples. An important aspect of these spatial statistics is that the variogram is influenced by the symmetry, structure and position of an object (e.g. a tree) within the scene (Zawadzki *et al.* 2005). Some authors have suggested the use of bidirectional variograms to take into account possible anisotropy.

In order to extract the spatial statistics, it is necessary to define the size of the moving window applied to the orthophoto image, obtained according to a trade-off between accurate statistical modelling of the texture properties (which requires relatively large window sizes) and undesired boundary effects (which increase by increasing the window size). More specifically, if too small a number of samples is considered, it may be insufficient for the generation of a statistically significant variogram, thus affecting the classification accuracy (Zawadzki *et al.* 2005). On the other hand, if too large a window is considered, the resulting border effects may decrease the classification accuracy significantly (Coburn and Roberts 2004).

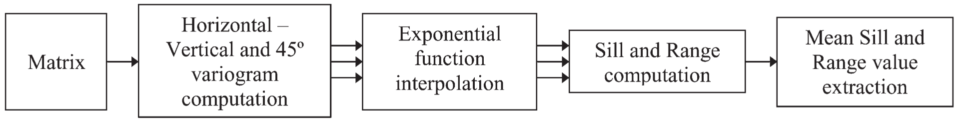


Figure 2. Scheme of the texture extraction process of the sill and range parameters from a matrix.

Figure 2 shows the scheme adopted for the extraction of the texture parameters from a window centred on a generic pixel of the image from which a matrix of digital numbers was extracted. Several simulations were carried out with different window sizes (from $13\times13$ to $55\times55$), and the resulting texture features were analysed (see figure 3). On the basis of this analysis, a window size equal to $23\times23$ pixels was selected in order to satisfy the above-mentioned trade-off. This is in agreement with the results obtained by Chen and Gong (2004). Multidirectional (horizontal, vertical and diagonal directions) variograms were evaluated from each matrix according to the previous equation, using a lag value of 17. The samples obtained were then interpolated with an exponential function (Bruniquel-Pinet and Gastellu-Etchegorry 1998). For the interpolation process, the convergence was evaluated using the nonlinear optimization algorithm proposed by Hooke and Jeeves (1961), which is based on the minimization of the mean-squared error. In this study the sill is associated with the horizontal asymptote value and the range corresponds to the distance at which 99.9% of the sill is reached. The average range and sill of the resulting omnidirectional variogram were then calculated to obtain a one-dimensional conventional structure. The extracted semivariogram parameters were assigned to each pixel (the central pixel of the window) and organized into additional layers.

Figure 4 shows the overall data-processing protocol. Starting from the orthophoto, the maps of sill and range were generated using a moving window for texture computation. For each matrix, a sill and range value was extracted. The mobile window size was then varied, using a step of five pixels to create the texture maps,

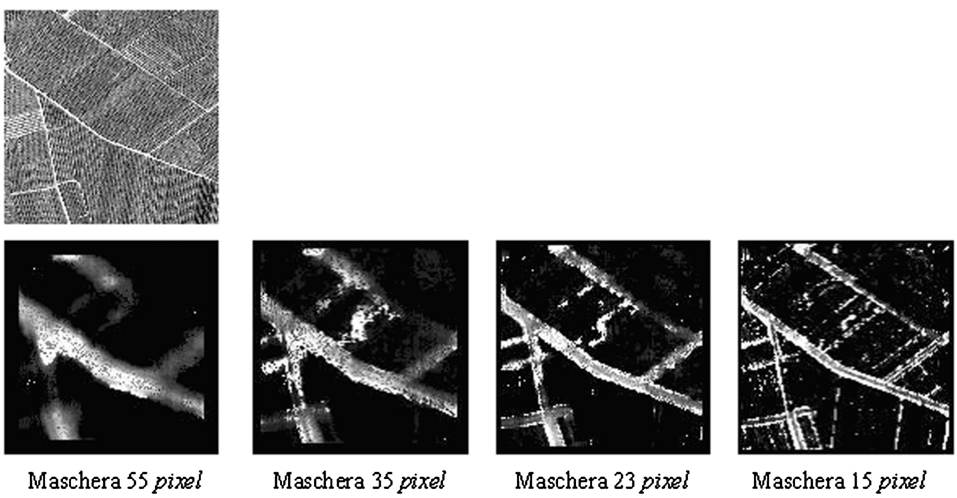


Figure 3. Examples of range maps obtained by using different sizes of the moving window. The image size is $0.25\times0.25$ km.

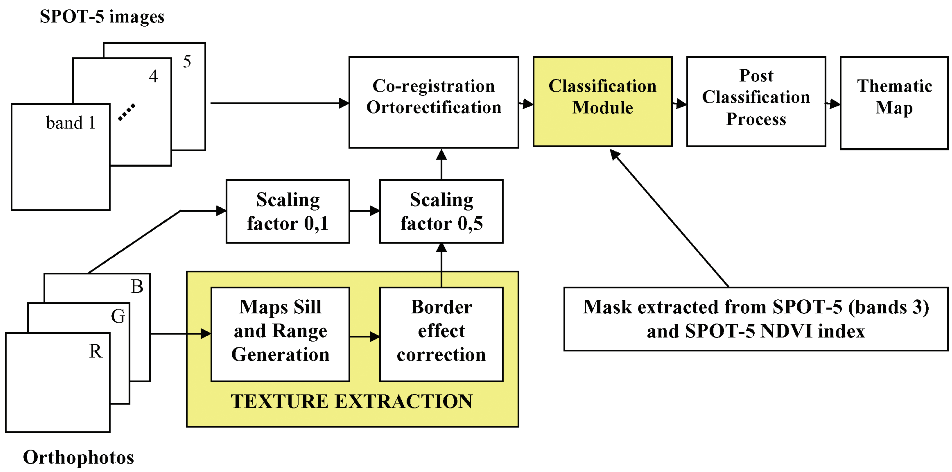


Figure 4. Overall data-processing chain.

scaling by a factor of two to the 10 m resolution of the SPOT-5 images. A median filter with a window size of $5 \times 5$ pixels was applied to reduce noise in the images and a morphological filter in the modality 'erode' was used to smooth and reduce the small bright regions corresponding to the areas with maximum values of range (e.g. streets, buildings and rocks). A visual analysis confirms that the filtering approach increases the accuracy of details and, in particular, reduces the so-called 'edge effects', which can lead to the misclassification of border areas or to an overestimation of classification accuracy for some features (Coburn and Roberts 2004). This is especially true when the boundary of the feature tends to dilate and to encompass the ground data, as in the case of streets and rocks. All the data processing was performed automatically by a C++ specifically developed program.

## 3. Experimental results

### 3.1 *Experimental design*

For all experiments, a standard maximum likelihood classification technique was used. The land-cover classes considered in the trials were forest, crops, grassland or pasture, open space (e.g. artificial structures, streets or rocks), water (e.g. rivers and mountain lakes) and shadow (small areas without illumination and a small reflectance value). Samples belonging to each class were selected visually from the orthophotos using the original 1 m resolution image for the definition of their labels. In order to limit the effect of possible mis-registration errors, the samples were collected from areas made up of clusters of pixels belonging to the same land-cover class. According to this strategy, 60–80 samples for each class for classifier training were selected, while an additional 200 samples were used to validate the accuracy of the classifier. To distinguish between the urban zone and the other non-vegetation classes, two filter masks were tested; the first one based on the red band of the orthophoto, and the second one based on the NDVI calculated from the second and third bands of the SPOT-5 images (figure 5). The first mask was chosen, as the second tended to eliminate rocky zones, which were misinterpreted as grassland.

Pixel-based classification maps are not homogeneous since the classification technique only partially includes the spatial context information in which the pixel is

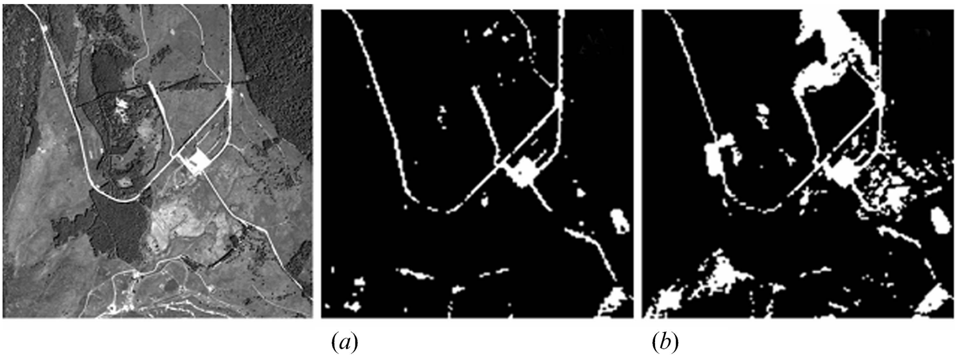


Figure 5. Original image and mask obtained from (*a*) orthophoto and (*b*) NDVI index. The image size is $1.5 \times 1.5$ km.

located. A correct regularization of the maps can be obtained by applying a simple majority analysis, which allows replacement of spurious pixels with the class label for the majority of the pixels in the kernel. The effect of majority analysis (which replaces spurious pixels with the value of the closest class in the post-processing analysis) and its potential to increase the automatic integrated classification accuracy was analysed.

### 3.2 *Results: texture features*

Different behaviours of a mono-directional variogram for the four different classes were observed (figure 6). The shape of the variogram provides information about the structure on the ground. For example, in the crops variogram, a strong cyclical trend caused by the periodicity of the elements is evident, due to the regular disposition of the rows in the analysed crops. In addition, the height of the sinusoidal curve is correlated with the distance between the rows. The curve changes

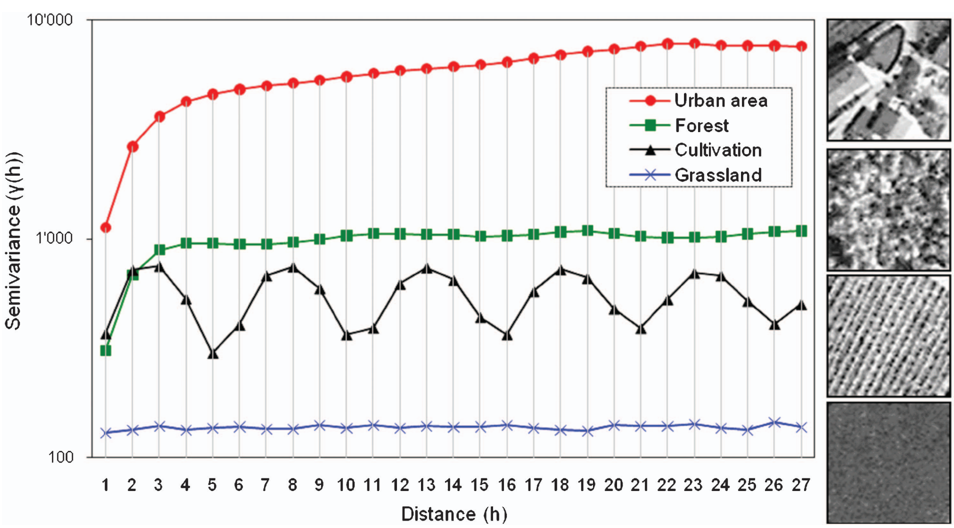


Figure 6. Semivariograms of training sites evaluated in a single direction and in a logarithmic scale. The spatial variability is visible for four different cover-types: forest, crops, grassland and urban areas.

its periodicity depending on the angle between the row direction and the direction at which the variogram is calculated. As mentioned previously, an exponential function for the interpolation of samples was used; however, in this particular situation, a periodic model using a trigonometric function was more appropriate. The variogram associated with the urban zone has a large variance, and the shape is irregular. This behaviour is caused by the presence of several objects (trees, streets and buildings) with different patterns within the same region of interest. In contrast, the forest presented a unique pattern and generated a variogram where the semivariance value increases regularly with the increase of the lag, tending to a horizontal asymptote, probably as a result of isotropy. In fact, the structural disposition of forest parameters, such as the mean, variance, sill, range and, thus, the autocorrelation, are the same in all directions. The semivariogram shape associated with grassland is characterized by a linear horizontal plane and is associated with very small semivariance values (figure 6).

The C++ program was used for semivariogram extraction in order to build complete maps at a 5 m resolution for each parameter. Figure 7(*a*) shows that the range values were very small for crops due to the highly regular pattern that characterizes these zones. The range values associated with forest (figure 7(*b*)) were higher than those for crops, and are represented on the map by different grey scales. The values increased when forest cover is low (due to reduced stem density) and when the mean dimension of the trees increased. These values are influenced by the light conditions, as demonstrated by many studies based on the use of simulated vegetation models (Bruniquel-Pinet and Gastellu-Etchegorry 1998). In the case of grassland, the range value increased, and was sometimes influenced by the presence



(*a*)

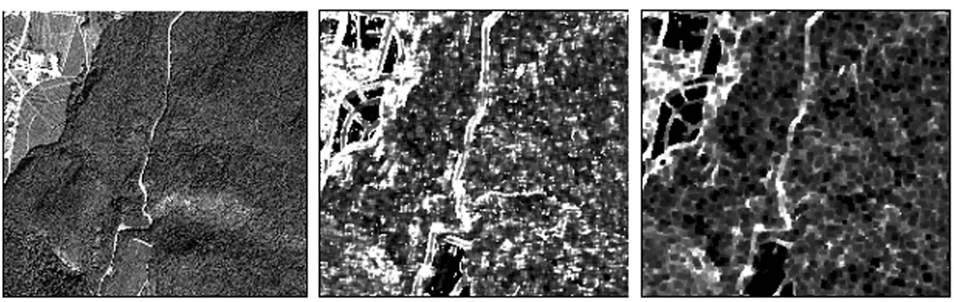

(*b*)

Figure 7. Original orthophoto and range maps before and after morphological correction for two different land-cover classes: (*a*) crops and (*b*) forest. The image size is 1 km × km.

of rocky areas (which are typical of a mountain landscape). The range value corresponding to all the other classes tended to saturate and, consequently, all the artificial structures, such as streets and towns, appear white (figure 7). Figure 7 also shows the reduction of the edge effect obtained with the application of morphological filtering and indicates that this method provides a reasonable reconstruction of the original area. Similar results were obtained when correcting for edge effects between forests and urban zones (figure 7(*b*)).

### 3.3 *Results: classification maps*

In figure 8, a visual comparison of the map obtained with conventional multi-spectral classification and that generated with the method proposed in this study is given. Although the training set used in the supervised classification procedure was identical for all maps, standard classification techniques incorrectly classified many pixels belonging to forest and grassland as crops. The use of textural information reduced the errors, leading to a better detection of large grassland areas (figure 8(*a*)).

Texture information was particularly helpful for distinguishing grasslands and forests from crops. Using the SPOT-5 information alone, 255 pixels of crops were misclassified as grassland; however, when texture information was added, the number of misclassified pixels decreased to 110. Similarly, by integrating texture information, the number of pixels of crops classified as forest decreased from 233 to 38. This misclassification is due to the fact that orchards (belonging to the crop class) tend to be mismatched as deciduous forests, because of their rather analogous spectral characteristics and canopy structure. For the same reason, herbaceous crops (such as maize) tend to be misclassified as grassland. Also, due to the high percentage of grass coverage typical of local vineyards, these crops can be

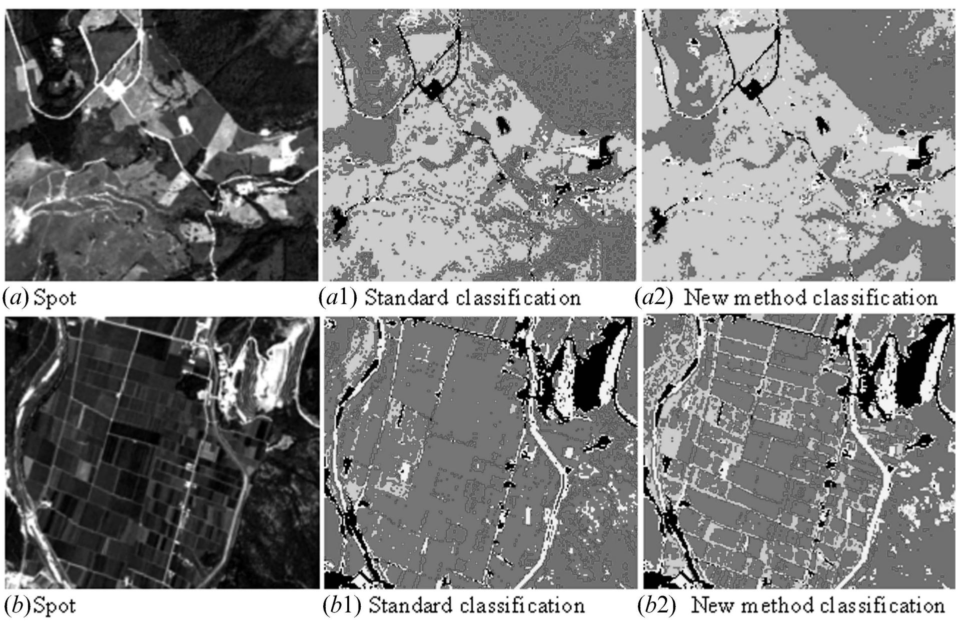


Figure 8. Portion of the original SPOT-5 image referring to (*a*) grassland and (*b*) crops. Comparison between classification maps obtained by using (1) standard multi-spectral features and (2) textural features. The image size is $2 \times 2$ km.

Table 1. Classification accuracy using spectral and texture features.

| Information sources | Classification approach | Kappa coefficient | User accuracy (%) |
|---|---|---|---|
| Orthophoto | Multi-spectral classification | 0.670 | 76.3 |
| Orthophoto + Texture | Texture integrated classification | 0.733 | 80.4 |
| SPOT | Multi-spectral classification | 0.822 | 87.5 |
| SPOT + Texture | Texture integrated classification | 0.887 | 92.1 |
| Orthophoto + SPOT + Texture | Texture integrated classification | 0.889 | 92.2 |

misclassified easily as grassland. Considering the obvious spatial patterns typical of vineyards, orchards and herbaceous crops, it is possible to understand the importance of texture, especially in a complex environment where topography and fragmented landscapes can affect the reflectance response heavily.

Figure 8(*b*) shows a specific subset of the SPOT-5 image related to an agricultural zone. Here, the texture information introduced as input to the classifier increased the detection of agricultural classes. In this case, it is clear that many pixels belonging to the forest class were classified correctly only in the second map, which was integrated with texture data.

In order to quantitatively analyse the generated classification maps, the class statistics and the confusion matrix of each classification result were analysed on the 200 test samples (see table 1). A general increase in accuracy was achieved when texture information was included in the analysis. Using the SPOT-5 multi-spectral features, the user's accuracy was equal to 87.5%. This value increased to 92.1% when the texture information was integrated with the SPOT-5 images. No increase in the accuracy values was observed when orthophoto spectral information (blue, green, red bands) was added to the above-mentioned set.

Tables 2 and 3 show the values of user accuracies (in percent) for each land-cover class, considering both the spectral information alone and the spectral features integrated with the texture data extracted from the orthophoto. For crops, the accuracy increased from 68.9% to 87.9%, indicating that recognition of spatial patterns plays a fundamental role in crop classification. In fact, when spectral information alone was used, many pixels belonging to forest and grassland were classified incorrectly as crops, especially in the transition zones (figure 8). In

Table 2. Error matrix using the multi-spectral information.

| | Forest | Crops | Grassland | Urban zone | User's accuracy (%) |
|---|---|---|---|---|---|
| Forest | 2382 | 2 | 0 | 0 | 99.5 |
| Crops | 233 | 1183 | 255 | 20 | 68.9 |
| Grassland | 3 | 93 | 691 | 3 | 86.8 |
| Urban zone | 0 | 46 | 0 | 489 | 91.1 |
| Producer's accuracy (%) | 91.0 | 89.4 | 73.0 | 93.3 | |
| Overall accuracy (4967/5679) | | | 87.5% | | |
| Kappa coefficient | | | 0.822 | | |

Table 3. Error matrix using both multi-spectral and texture features.

| | Forest | Crops | Grassland | Urban zone | User's accuracy (%) |
|---|---|---|---|---|---|
| Forest | 2539 | 6 | 3 | 0 | 99.2 |
| Crops | 38 | 1145 | 110 | 1 | 87.9 |
| Grassland | 13 | 120 | 828 | 12 | 83.5 |
| Urban zone | 13 | 53 | 0 | 492 | 87.9 |
| Producer's accuracy (%) | 97.0 | 86.5 | 87.5 | 93.9 | |
| Overall accuracy (5229/5679) | | | 92.1% | | |
| Kappa coefficient | | | 0.887 | | |

contrast, the grassland class showed a slight decrease in accuracy (from 86.9% to 83.5%). The forest accuracy values were very high in both cases (99.5% vs. 99. 7%), while the urban zone showed a slight decrease in accuracy (from 91.1% to 87.9%).

The accuracies obtained before and after the use of simple majority analysis are shown in table 4. When simple majority analysis was used in the SPOT-5 image alone, it produced a slight increase in accuracy for both the grassland class (from 86.8% to 91.4%) and the crop class (from 68.9% to 72.2%). For grassland classification, the use of simple majority analysis was more effective than the integration of textural information. In such ecosystems, in fact, the spatial information related to natural heterogeneity, landscape fragmentation and extreme morphological complexity is not as relevant as in crops.

Using a simple majority analysis of the SPOT-5 image integrated with texture information, more accurate results were obtained for crops (accuracy increased from 87.9% to 98.2%), while grassland areas showed a slight decrease in accuracy (from 91.4% to 87.0%) when compared to the majority analysis alone.

The overall accuracy deriving from the majority analysis applied to the SPOT-5 image integrated with texture information was equal to 94.6%, with a kappa coefficient of 0.923.

## 4. Conclusion

The results obtained in the experimental analysis presented in this paper suggest that the combination of the majority analysis and the proposed automatic classification strategy is an effective approach when dealing with highly fragmented and complex Alpine landscapes.

Table 4. Classification accuracy before and after the use of a post-processing technique based on a majority analysis.

| | Pixel based | | Majority analysis | |
|---|---|---|---|---|
| Classification procedure | Kappa coefficient | User accuracy (%) | Kappa coefficient | User accuracy (%) |
| SPOT multi-spectral classification | 0.822 | 87.5 | 0.850 | 89.5 |
| Texture integrated classification | 0.887 | 92.1 | 0.923 | 94.6 |

Table 5. Error matrix obtained by using only the multi-spectral information after the use of majority analysis.

| | Forest | Crops | Grassland | Urban zone | User's accuracy (%) |
|---|---|---|---|---|---|
| Forest | 2457 | 0 | 0 | 0 | 99.7 |
| Crops | 161 | 1209 | 245 | 20 | 72.2 |
| Grassland | 0 | 65 | 701 | 0 | 91.4 |
| Urban zone | 0 | 50 | 0 | 500 | 90.6 |
| Producer's accuracy (%) | 93.9 | 91.3 | 74.1 | 95.4 | |
| Overall accuracy (5082/5679) | | | 89.5% | | |
| Kappa coefficient | | | 0.850 | | |

Error matrices for the different land uses obtained by using the multi-spectral information alone or both spectral and textural information (after the use of majority analysis) are shown in tables 5 and 6. Spatial information extracted by semivariogram texture analysis increased the capability of detection of the different vegetation classes, particularly for crops, which often have a regular spatial pattern. On the contrary, the results indicate that for grassland ecosystems, the spatial information related to natural heterogeneity and extreme morphological complexity is not as useful for classification as in crops. Overall, using multi-spectral classification alone the classification accuracy was equal to 87.5%, but it increased to 92.1% when texture information was included in the analysis. In addition, by using a simple majority analysis, even more accurate results could be obtained (up to 94.6%, with a kappa coefficient of 0.923). In this case, also the accuracy on grassland, crops and urban zones increased.

It should be noted that the increase in accuracy related to the texture analysis is achieved by using a parametric maximum likelihood approach, which can exploit the information present in texture features only partially due to the approximation with a Gaussian model of the distribution of texture measures (Bruzzone *et al.* 1997). Therefore, more studies are needed in order both to explore the effect of transforming the distribution of the texture features to normality (Chen and Gong 2004), and to use other non-parametric classifiers (e.g. neural networks, support vector machines) to increase the total information obtained with texture features extracted from orthophotos.

According to the results, it is possible to conclude that our integrated approach increased the accuracy of the classification process of the considered complex

Table 6. Error matrix obtained by using both the multi-spectral and the texture features after the use of majority analysis.

| | Forest | Crops | Grassland | Urban zone | User's accuracy (%) |
|---|---|---|---|---|---|
| Forest | 2604 | 0 | 0 | 0 | 99.58 |
| Crops | 2 | 1165 | 67 | 0 | 93.20 |
| Grassland | 5 | 109 | 879 | 2 | 87.03 |
| Urban zone | 2 | 50 | 0 | 502 | 90.29 |
| Producer's accuracy (%) | 99.5 | 88.0 | 92.9 | 95.8 | |
| Overall accuracy (5373/5679) | | | 94.6% | | |
| Kappa coefficient | | | 0.923 | | |

topography areas, leading to a reduction of costs and encouraging frequent updating of data.

## References


Atkinson, P.M. and Lewis, P., 2000, Geostatistical classification for remote sensing: an introduction. *Computers and Geosciences*, **26**, pp. 361–371.

Bruniquel-Pinel, V. and Gastellu-Etchegorry, J., 1998, Sensitivity of texture of high resolution images of forest to biophysical and acquisition parameters. *Remote Sensing of Environment*, **65**, pp. 61–85.

Bruzzone, L., Conese, C., Maselli, F. and Roli, F., 1997, Multisource classification of complex rural areas by statistical and neural-network approaches. *Photogrammetric Engineering & Remote Sensing*, **63**, pp. 523–533.

Butson, C. and King, D., 1999, Semivariance analysis of forest structure and remote sensing data to determine an optimal sample plot size. *Proceedings of Fourth International Airborne Remote Sensing Conference and Exhibition*, Ottawa, Ontario, 21–24 June, pp. 155–162.

Chen, Q. and Gong, P., 2004, Automatic variogram parameter extraction for textural classification of the panchromatic IKONOS imagery. *GeoRS*, **42**, pp. 1106–1115.

Coburn, C.A. and Roberts, A.C.B., 2004, A multiscale texture analysis procedure for improved forest stand classification. *International Journal of Remote Sensing*, **25**, pp. 4287–4308.

Cohen, W.B., Spies, T.A. and Bradshaw, T.A., 1990, Semivariograms of digital imagery for analysis of conifer canopy structure. *Remote Sensing of Environment*, **34**, pp. 167–178.

Colombo, R., Bellingeri, D., Fasolini, D. and Marino, C., 2003, Retrieval of leaf area index in different vegetation types using high resolution satellite data. *Remote Sensing of Environment*, **86**, pp. 120–131.

Curran, P.J., 1998, The semivariogram in remote sensing: an introduction. *Remote Sensing of Environment*, **24**, pp. 493–507.

Dreyer, P., 1993, Classification of land cover using optimized neural nets on SPOT data. *Photogrammetric Engineering and Remote Sensing*, **59**, pp. 617–621.

Franklin, S., Wulder, M. and Lavigne, M., 1996, Automated derivation of geographic windows sizes for use in remote sensing digital image texture analysis. *Computers & Geosciences*, **22**, pp. 665–673.

Goodenough, D.G., Dyk, A., Niemann, K.O., Pearlman, J.S., Chen, H., Han, T., Murdoch, M. and West, C., 2003, Processing Hyperion and ALI for forest classification. *IEEE Transactions on Geoscience and Remote Sensing*, **41**, pp. 1321–1331.

Hese, S., 2001, Segmentation of forest stand in very high resolution stereo data. *Geoscience and Remote Sensing Symposium, IEEE 2001 International*, **4**, pp. 1654–1656.

Hooke, R. and Jeeves, T.A., 1961, Direct search solution of numerical and statistical problems. *Journal of the ACM*, **8**, pp. 212–229.

Hsu, S.Y., 1978, Texture-Tone analysis for automated Land-use mapping. *Photogrammetric Engineering and Remote Sensing*, **44**, pp. 1393–1404.

Hudak, A.T. and Wessman, C.A., 1998, Textural analysis of historical aerial photography to characterize woody plant encroachment in South African Savanna. *Remote Sensing of Environment*, **66**, pp. 317–330.

Hudak, A.T. and Wessman, C.A., 2001, Textural analysis of high resolution imagery to quantify bush encroachment in Madikwe Game Reserve, South Africa, 1955–1996. *International Journal of Remote Sensing*, **22**, pp. 2731–2740.

Hyde, P., Dubayah, R., Walker, W., Blair, J.B., Hofton, M. and Hunsaker, C., 2006, Mapping forest structure for wildlife habitat analysis using multi-sensor (LiDAR, SAR/InSAR, ETM+, Quickbird) synergy. *Remote Sensing of Environment*, **102**, pp. 63–73.

LÉVESQUE, J. and KING, D., 1999, Airborne digital camera image semivariance for evaluation of forest structural damage at an acid mine site. *Remote Sensing of Environment*, **68**, pp. 112–124.

LÉVESQUE, J. and KING, D., 2003, Spatial analysis of radiometric fractions from high-resolution multi-spectral imagery for modelling individual tree crown and forest canopy structure and health. *Remote Sensing of Environment*, **84**, pp. 859–602.

LU, D. and WENG, Q., 2007, A survey of image classification methods and techniques for improving classification performance. *International Journal of Remote Sensing*, **28**, pp. 823–870.

MIRANDA, F.P. and FONSECA, L.E.N., 1998, Semivariogram textural classification of JERS-1 (Fuyo-1) SAR data obtained over a flooded area of the Amazon rainforest. *International Journal of Remote Sensing*, **19**, pp. 549–556.

NEL, E.M., WESSMAN, C.A. and VEBLEN, T.T., 1994, Digital and visual analysis of Thematic Mapper imagery for differentiating old growth from younger spruce-fir stands. *Remote Sensing of Environment*, **48**, pp. 291–301.

RUIZ, L.A., FDEZ-SARRIA, A. and RECIO, J.A., 2004, Texture feature extraction for classification of remote sensing data using wavelet decomposition: a comparative study. In *Proceedings of the 20th ISPRS Congress, IAPSR Vol. XXXV (B4)*, Istanbul, Turkey, pp. 1109–1114.

SEDANO, F., GONG, P. and FERRAO, M., 2005, Land cover assessment with MODIS imagery in southern African Miombo ecosystems. *Remote Sensing of Environment*, **98**, pp. 429–441.

ST-ONGE, B. and CAVAYAS, F., 1995, Estimating forest stand structure from high resolution imagery using the directional semivariogram. *International Journal of Remote Sensing*, **16**, pp. 1999–2021.

ST-ONGE, B. and CAVAYAS, F., 1997, Automated forest structure mapping from high resolution imagery based on directional semivariogram estimates. *Remote Sensing of Environment*, **61**, pp. 82–95.

WULDER, M., FRANKLIN, S. and LAVIGNE, M., 1996, Statistical texture proprieties of forest structure for improved estimates of LAI from CASI. In *Proceedings of the 26th International Symposium on Remote Sensing of the Environment and 18th Annual Symposium of the Canadian Remote Sensing Society*, Vancouver, pp. 111–164.

WULDER, M., LEDREW, E., FRANKLIN, S. and LAVIGNE, M., 1998, Aerial image textural information in the estimation of northern deciduous and mixed wood forest Leaf Area Index. *Remote Sensing of Environment*, **64**, pp. 64–76.

ZAWADZKI, J., CIESZEWSKI, C.J., ZASADA, M. and LOWE, R.C., 2005, Applying geostatistics for investigations of forest ecosystems using remote sensing imagery. *Silva Fennica*, **39**, pp. 599–616.

ZHANG, C., FRANKLIN, S.E. and WULDER, M.A., 2004, Geostatistical and texture analysis of airborne-acquired images used in forest classification. *International Journal of Remote Sensing*, **25**, pp. 859–865.

ZHANG, Y., 2001, A spectral and spatial information integrated approach for tree extraction from high-resolution digital imagery. In *Beyond Information Infrastructure, Proceedings of the Digital Earth 2001 Conference*, Fredericton, 24–28 June.